Beam bending via plasmonic lenses

Yanhui Zhao, Sz-Chin Steven Lin, Ahmad Ahsan Nawaz, Brian Kiraly, Qingzhen Hao, Yanjun Liu and Tony Jun Huang*

Department of Engineering Science and Mechanics, Pennsylvania State University, State College, Pennsylvania 16802, USA

**junhuang@engr.psu.edu*

Abstract: We have designed and characterized three different types of plasmonic lenses that cannot only focus, but can also bend electromagnetic (EM) waves. The bending effect is achieved by constructing an asymmetric phase front caused by varying phase retardations in EM waves as they pass through a plasmonic lens. With an incident wave normal to the lens surface, light bends up to 8° off the axial direction. The optical wave propagation was numerically investigated using the finite-difference time-domain (FDTD) method. Simulation results show that the proposed plasmonic lenses allow effective beam bending under both normal and tilted incidence. With their relatively large bending range and capability to perform in the far field, the plamsonic lenses described in this article could be valuable in applications such as photonic communication and plasmonic circuits.

OCIS codes: (240.6680) Surface plasmons; (050.6624) Subwavelength structures.

References and links

1. M. Born, and E. Wolf, *Principle of Optics*, Seventh Edition, Cambridge University Press, 1999.
2. Z. Liu, J. M. Steele, W. Srituravanich, Y. Pikus, C. Sun, and X. Zhang, "Focusing surface plasmons with a plasmonic lens," Nano Lett. **5**(9), 1726–1729 (2005).
3. W. Srituravanich, L. Pan, Y. Wang, C. Sun, D. B. Bogy, and X. Zhang, "Flying plasmonic lens in the near field for high-speed nanolithography," Nat. Nanotechnol. **3**(12), 733–737 (2008).
4. C. K. Chang, Y. Y. Yu, M. W. Lai, J. T. Yeh, J. M. Liu, C. S. Yeh, and C. K. Lee, "Recording Bessel-like beam shapes generated by plasmonics lens," Opt. Express **17**(16), 13946–13952 (2009), http://www.opticsinfobase.org/abstract.cfm?URI=oe-17-16-13946.
5. G. M. Lerman, A. Yanai, and U. Levy, "Demonstration of nanofocusing by the use of plasmonic lens illuminated with radially polarized light," Nano Lett. **9**(5), 2139–2143 (2009).
6. J. A. Shackleford, R. Grote, M. Currie, J. E. Spanier, and B. Nabet, "Integrated plasmonic lens photodetector," Appl. Phys. Lett. **94**(8), 083501 (2009).
7. Y. Fu, Y. Liu, X. Zhou, Z. Xu, and F. Fang, "Experimental investigation of superfocusing of plasmonic lens with chirped circular nanoslits," Opt. Express **18**(4), 3438–3443 (2010), http://www.opticsinfobase.org/abstract.cfm?URI=oe-18-4-3438.
8. H. A. Atwater, "The promise of plasmonics," Sci. Am. **296**(4), 56–62 (2007).
9. L. Martin-Moreno, "Plasmonic circuits: Detecting unseen light," Nat. Phys. **5**(7), 457–458 (2009).
10. W. Chen, D. C. Abeysinghe, R. L. Nelson, and Q. Zhan, "Experimental confirmation of miniature spiral plasmonic lens as a circular polarization analyzer," Nano Lett. **10**(6), 2075–2079 (2010).
11. S. Yang, W. Chen, R. L. Nelson, and Q. Zhan, "Miniature circular polarization analyzer with spiral plasmonic lens," Opt. Lett. **34**(20), 3047–3049 (2009), http://www.opticsinfobase.org/abstract.cfm?URI=ol-34-20-3047.
12. B. Lee, S. Kim, H. Kim, and Y. Lim, "The use of plasmonics in light beaming and focusing," Prog. Quantum Electron. **34**(2), 47–87 (2010).
13. H. Shi, C. Du, and X. Luo, "Focal length modulation based on a metallic slit surrounded with grooves in curved depths," Appl. Phys. Lett. **91**(9), 093111 (2007).
14. L. Verslegers, P. B. Catrysse, Z. Yu, J. S. White, E. S. Barnard, M. L. Brongersma, and S. Fan, "Planar lenses based on nanoscale slit arrays in a metallic film," Nano Lett. **9**(1), 235–238 (2009).
15. L. Lin, X. M. Goh, L. P. McGuinness, and A. Roberts, "Plasmonic lenses formed by two-dimensional nanometric cross-shaped aperture arrays for Fresnel-region focusing," Nano Lett. **10**(5), 1936–1940 (2010).
16. S. Kim, H. Kim, Y. Lim, and B. Lee, "Off-axis directional beaming of optical field diffracted by a single subwavelength meatl slit with asymmetric dielectric surface gratings," Appl. Phys. Lett. **90**(5), 051113 (2007).
17. Z. Liu, J. M. Steele, H. Lee, and X. Zhang, "Tuning the focus of a plasmonic lens by the incident angle," Appl. Phys. Lett. **88**(17), 171108 (2006).
18. S. I. Bozhevolnyi, V. S. Volkov, E. Devaux, J. Y. Laluet, and T. W. Ebbesen, "Channel plasmon subwavelength waveguide components including interferometers and ring resonators," Nature **440**(7083), 508–511 (2006).

#134990 - $15.00 USD Received 13 Sep 2010; revised 11 Oct 2010; accepted 15 Oct 2010; published 22 Oct 2010

19. E. Verhagen, A. Polman, and L. K. Kuipers, "Nanofocusing in laterally tapered plasmonic waveguides," Opt. Express **16**(1), 45–57 (2008), http://www.opticsinfobase.org/oe/abstract.cfm?URI=oe-16-1-45.
20. D. F. P. Pile, and D. K. Gramotnev, "Channel plasmon-polariton in a triangular groove on a metal surface," Opt. Lett. **29**(10), 1069–1071 (2004), http://www.opticsinfobase.org/abstract.cfm?URI=ol-29-10-1069.
21. T. Søndergaard, S. I. Bozhevolnyi, S. M. Novikov, J. Beermann, E. Devaux, and T. W. Ebbesen, "Extraordinary optical transmission enhanced by nanofocusing," Nano Lett. **10**(8), 3123–3128 (2010).
22. G. I. Stegeman, R. F. Wallis, and A. A. Maradudin, "Excitation of surface polaritons by end-fire coupling," Opt. Lett. **8**(7), 386–388 (1983), http://www.opticsinfobase.org/abstract.cfm?URI=ol-8-7-386.
23. R. Gordon, and A. G. Brolo, "Increased cut-off wavelength for a subwavelength hole in a real metal," Opt. Express **13**(6), 1933–1938 (2005), http://www.opticsinfobase.org/oe/abstract.cfm?URI=oe-13-6-1933.
24. Z. Sun, and H. K. Kim, "Refractive transmission of light and beam shaping with metallic nano- optic lenses," Appl. Phys. Lett. **85**(4), 642–644 (2004).
25. Mathematica 7.0, licensed to ESM department, Penn State University. http://www.wolfram.com/
26. Y. Fu, W. Zhou, L. E. N. Lim, C. L. Du, and X. G. Luo, "Plasmonic microzone plate: Superfocusing at visible regime," Appl. Phys. Lett. **91**(6), 061124 (2007).
27. F. D. T. D. Optiwave, 8.0, licensed to BioNEMS group, Penn State Univ. http://www.optiwave.com/
28. P. B. Johnson, and R. W. Christy, "Optical Constants of the Noble Metals," Phys. Rev. B **6**(12), 4370–4379 (1972).
29. H. Raether, (1988). *Surface plasmons on smooth and rough surfaces and on gratings.* Springer Verlag, Berlin. ISBN 978–3540173632.
30. Image Processing and Analysis in Java (ImageJ). *http://rsbweb.nih.gov/ij/*
31. J. A. Kong, *Electromagnetic Wave Theory*, EMW Publishing, 2005.

1. Introduction

With the advent of nanotechnology, the ever-increasing interest to explore the optical world at nanoscale has presented the demand to manipulate visible light in the subwavelength scale. Researchers have made significant efforts to decrease the size of optical lenses to micron and submicron scale for this very purpose; however, due to diffraction limit [1], their efforts are hindered when the size of a lens approaches the wavelength of the light. One possible method that enables the manipulation of visible light in the subwavelength scale uses surface plasmons; these surface plasmon-based lenses, or so-called plasmonic lenses, can achieve subwavelength-scale focal zones [2–7]. Plasmonic lenses have proven to be useful in numerous applications such as nanofabrication [2–4], nanophotonic circuits [6, 8, 9], and circular polarizer analyzers [10, 11]. In these applications, plasmonic lenses have been used to focus light at subwavelength scale. However, to fully realize the potential of plasmonic lenses, it is necessary to not only focus light, but also to manipulate and precisely position it at small scales [12].

Positional modulation through a plasmonic lens was first numerically demonstrated in Shi's study [13], where an axial tuning of the focal points was obtained by varying depths of grooves surrounding a central slit. Experimental demonstrations of the same concept have been reported by Verslegers *et al.* [14] and Lin *et al.* [15], independently. Meanwhile, little work has been done to achieve directional tuning (*i.e.*, bending) of light through a plasmonic lens. Kim *et al.* constructed an asymmetric metallic plasmonic lens with different materials to deflect normally incident light beams; unfortunately, the limited choices of high refractive index dielectric materials and requirement of multilayer fabrication process severely compromise the applicability of this approach [16]. Liu *et al.* tuned the focal point off the optical axis simply by changing the incident angle of the incident light beam [17]; however, in this approach, the tuning occurs only in the near field, which significantly restricts the working distance.

In this article, we aim to provide a more practical, easy-to-implement method to achieve directional modulation with a plasmonic lens. We introduce a design principle for plasmonic lenses that can bend light along the direction transverse to the propagation direction. Light bending is achieved by constructing a carefully designed, curved phase front for the plasmonic lenses. The control of the phase front profile is achieved through two mechanisms: phase retardation caused by the width and shape of the individual slits in the lens, and the

#134990 - $15.00 USD Received 13 Sep 2010; revised 11 Oct 2010; accepted 15 Oct 2010; published 22 Oct 2010

position of these slits. The proposed single-layered lenses can be conveniently fabricated using Focused Ion Beam (FIB) techniques and are thus much more feasible than their existing counterparts. In addition, far-field intensity redistribution with acceptable energy loss is observed in the simulation results.

2. Principles

To bend normally incident electromagnetic (EM) beams off the optical axis, we have designed three plasmonic lens structures. As depicted in Fig. 1, these designs (referred as Lens I, Lens II, and Lens III) are all composed of a linear array of air-filled rectangular or tapered slits in a gold or silver background. In Lens I, we use the dependence of phase change on slit width to our advantage. As shown in the design (Fig. 1(b)), the slit length d and spacing a are kept constant, while the slit width w along the transverse direction (y-axis) is varied. In Lens II (Fig. 1(c)), we design a slanted cut on the output side, which causes a linear variation of the slit length d from one end of the lens to another. The slit width (50 nm) and spacing are kept constant. In this case, although the transmission coefficient β is the same for all slits, different phase delays can be obtained by the dependency of phase change on slit length.

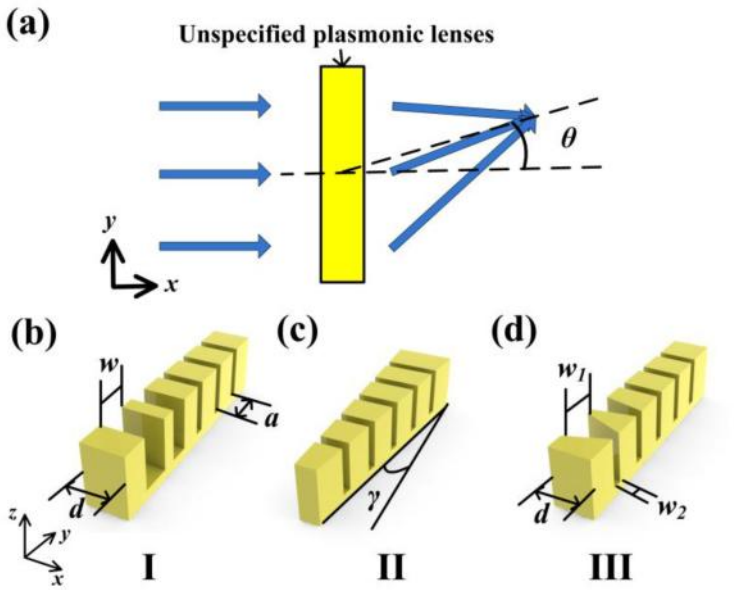

Fig. 1. (a) Schematic of a plasmonic lens that can bend a light beam or focal point in transverse direction; (b), (c) and (d) are the isometric views of three proposed designs of the plasmonic lens, termed as Lens I, Lens II, and Lens III.

In Lens III (Fig. 1(d)), we employ tapered slits to form an asymmetric phase front for beam bending, as tapered structures have proven useful in the design of plasmonic waveguides [18–20]. The main advantage of a tapered waveguide over a rectangular one lies in its superior surface plasmon mode confinement; this is because the output aperture of a tapered waveguide is generally smaller than the incident wavelength. The second advantage of using tapered structures is that enhanced transmission can be obtained when the input aperture is larger than the output aperture [21]. In the design of Lens III, we keep the slit length d, spacing a, and output aperture w_2 constant; the input aperture w_1 is the only variable in the design. Compared with the planar lens structure (Lens I), the tapered structure (Lens III) is expected to perform better in confining plasmonic modes and enhancing optical transmission.

#134990 - $15.00 USD Received 13 Sep 2010; revised 11 Oct 2010; accepted 15 Oct 2010; published 22 Oct 2010

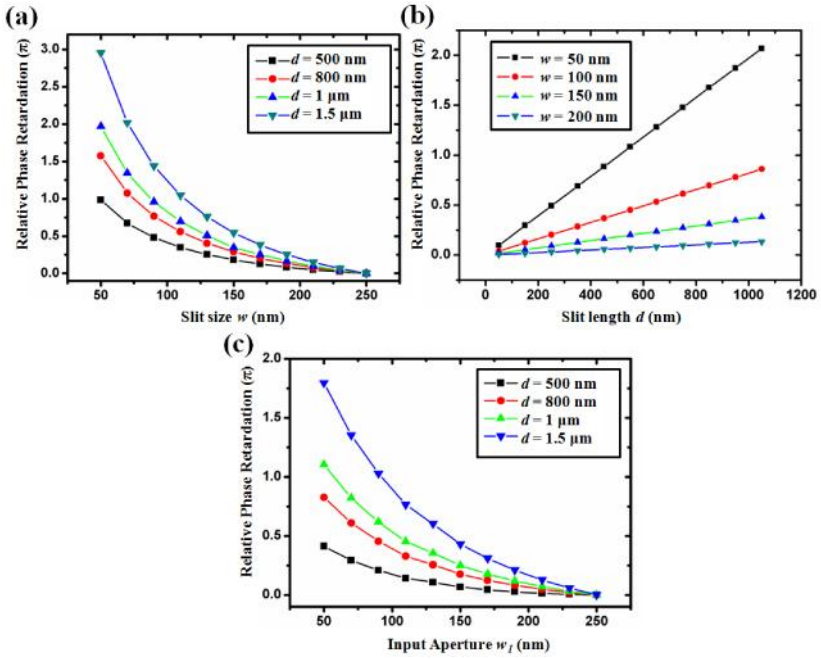

Fig. 2. (a) Relative phase change caused by varying the width of a rectangular slit *w*. (b) Relative phase difference caused by varying the length of the slit *d*. (c) Relative phase difference of a tapered slit. The input aperture w_1 is varying, while the output aperture w_2 is fixed at 50 nm.

In all three lens designs, each individual slit is significantly smaller than the incident wavelength; thus it can be treated as a plasmonic waveguide. As an incident EM wave meets the slits, it will be converted into surface plasmons due to the end-fire effect [22], transmitted in the form of surface plasmon modes along the waveguide, and then decoupled back to an EM mode with a phase delay upon exiting the slit. The transmission coefficient β, which is related to the phase change of the EM wave after it passes through the structure, can be expressed as [23, 24]:

$$\tan h(w\sqrt{\beta^2-\varepsilon_d k_0^2}/2) = -\frac{\varepsilon_d\sqrt{\beta^2-\varepsilon_m k_0^2}}{\varepsilon_m\sqrt{\beta^2-\varepsilon_d k_0^2}}, \quad (1)$$

where k_0 is the wave vector in vacuum, *w* is the aperture of the waveguide, and ε_d and ε_m are the permittivities of the dielectric material and metal, respectively. In the case of a tapered waveguide, the slit width *w* varies with propagation distance, and the transmission coefficient β varies accordingly. Nevertheless, we can calculate the effective transmission coefficient β_{eff} by integrating each discrete β along the length axis (*x*-axis) of a tapered waveguide. As the phase change, φ, of a plasmonic waveguide is the product of its transmission coefficient β and length *d* [14], its value can be controlled by varying β and *d* independently, which correspond to different channel lengths and widths respectively. Figure 2 illustrates the geometric dependencies of the phase change of a rectangular slit (Figs. 2(a) and (b)) and a tapered slit (Fig. 2(c)), calculated by using *Mathematica* [25]. We observe that the relative phase change φ is proportional to slit length (*d*) and inverse of slit width (1/*w*). As shown in Fig. 2(a), a relative value up to 3π can be obtained for φ as *w* increases from 50 nm to 250 nm, while *d* is kept at 1.5 μm. In Fig. 2(b), as the slit length d increases from 50 nm to 1050 nm, a linear increase in φ up to 2π can be observed when width of the slit is set at 50 nm. In Fig. 2(c), the relative phase difference of a tapered slit is plotted against its input aperture w_1, while the

#134990 - $15.00 USD Received 13 Sep 2010; revised 11 Oct 2010; accepted 15 Oct 2010; published 22 Oct 2010

output aperture w_2 is fixed at 50 nm for all conditions. The maximum relative phase shift is 1.8π when $d = 1.5$ μm.

The positional and directional modulation functionalities of a plasmonic lens are determined by the relative phase difference between neighboring slits. By introducing a continuous change to the slit geometry along the transverse direction (*x*-axis) of a plasmonic lens, we can create a relative phase difference profile across the width of the lens (*y*-axis). The position of the constructive interferences of the decoupled EM waves depends strongly on the phase delay profile, and it is expressed as beam modulation effect. In this article we focus on beam bending; thus we will build an asymmetric phase front across the plasmonic lens to achieve directional modulation.

Another factor that leads to a phase difference between neighboring slits is the spacing between the particular optical elements. We denote it as center-to-center distance *a* (Fig. 1). The center-to-center distance plays an important role in the design of Fresnel zone plates [1], in which focal points are located at the constructive interferences of the transmitted waves from circular slits. In a Fresnel zone plate, the phase difference between any two slits is $2n\pi$ and can be achieved by adjusting slit widths and inter-slit spacing. If we assume that the focal length of a zone plate is *f*, the phase difference between the center slit and a slit *m* units away can be expressed as [14]:

$$\varphi(m) = 2n\pi + \frac{2\pi f}{\lambda} - \frac{2\pi\sqrt{f^2 + m^2}}{\lambda}, \tag{2}$$

where λ is the incident wavelength and *n* is an integer. This design principle can be extended to the design of plasmonic lenses [26]. However, the radius of a plasmonic lens is merely several microns, so *n* cannot be large at all (at most 1 in our cases). Therefore, the phase difference caused by distances between slits will not play a dominant role in the design of the asymmetric plasmonic lens. In the approaches described in this article, we construct asymmetric phase front profiles by modulating the geometric parameters of slits, rather than adjusting inter-slit spacing.

3. Simulations and discussion

The EM wave propagation was simulated using commercial finite-difference time-domain (FDTD) software: Optiwave FDTD by Optiwave Systems Inc [27]. An area of 5 μm × 14 μm was chosen to study the effects of each proposed plasmonic lens structure. The boundary condition was set to the perfect electric condition (perfect matching layers) such that the transverse magnetic (TM) waves encountering these boundaries are totally absorbed. A mesh size of 5 nm × 5 nm was used to ensure convergent results. TM mode waves were used because of excitation requirements of the surface plasmon waves. The incident wavelength used was 633 nm, with the corresponding permittivity of metals at this wavelength calculated based on the Drude model [28]. For silver, the permittivity used was $-17.2355 + 0.4982i$. The center-to-center distance, *a*, of all the slits was set at 500 nm. It is worth noting that the distance between any two slits is much larger than the skin depth of surface plasmon inside the silver, which is of the order of tens of nanometers [29]; hence, no surface plasmon cross-talk will occur between adjacent slits. The length of the slit, or in other words, the thickness of the structure is another important parameter that, when increased, will cause a larger relative phase difference and corresponding modulating power. The trade-off of a thick structure is its low transmission due to high reflection at the interface and absorption inside the slit.

We first demonstrate beam deflection using the design of Lens I (Fig. 3(a)). The structure used in our simulation consists of an 800 nm thick sliver slab with seven slits whose width ranges from 50 nm to 200 nm (50 nm, 50 nm, 50 nm, 50 nm, 100 nm, 150 nm, 200 nm, from one side to the other), corresponding to a maximum phase difference of 1.5π. The phase front is presented by dashed lines in Fig. 3(a). Under normally incident radiation with a wavelength of 633 nm, two high-intensity regions can be observed: a farther one with a smaller off-axis

#134990 - $15.00 USD Received 13 Sep 2010; revised 11 Oct 2010; accepted 15 Oct 2010; published 22 Oct 2010

deflection angle refers to the main beam, and it is the beam we are interested. As for the strongest sidelobe with a higher deflection angle, it is not the focus of our discussion in this article. A main beam deflection of ~8° can be observed from the simulation due to the constructive interference of the phase-delayed, transmitted waves from the rectangular slits of Lens I (Fig. 3 (b)). The position of focus and the bending angle are determined using the image processing software, ImageJ [30], to capture the area with the highest intensity within the main beam. The locations of periphery lobes are determined by constructive interference conditions; however, all these sidelobes (including the strongest one) focus EM waves in the near field and do not contribute significantly to the plasmonic communication applications. We also show that Lens II with $\gamma = 3°$ can be used to deflect the light beam. In this design, the widths of all seven slits remain at 50 nm. In this slanted lens design, the slit length is varied linearly from 226 nm to 374 nm, corresponding to a phase difference of 0.96π. As illustrated in Fig. 3(d), the deflection angle of the main beam is observed to be around 3° with Lens II and the intensity of the focused beam is relatively low comparing to Lens I. The last design (Lens III, Fig. 3(e)) involves tapered slit structures with different input apertures. The output aperture width is kept at 50 nm, which ensures the confinement of surface plasmon modes inside the tapered structure, regardless of the width of input aperture. The widths of the input apertures are set to be 50 nm for the first four slits, and 100 nm, 150 nm, 200 nm for the last three slits, respectively. A phase difference of 1.45π is achieved, and the asymmetric phase front causes the light beam to bend 5° off the center axis and the focused beam is observed to have higher intensity than Lens I (Fig. 3(f)).

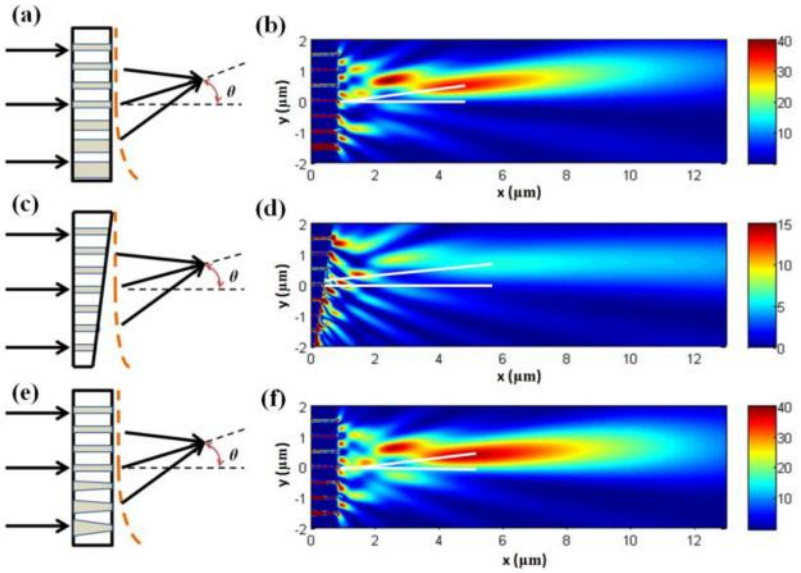

Fig. 3. (a), (c) and (e) are three representative designs of plasmonic lenses (Lens I, Lens II, Lens III), corresponding to Fig. 1(b), (c) and (d). The constructed phase differences are 1.5π, 0.96π, and 1.45π, respectively. (b), (d) and (f) the corresponding simulation results. All the simulations show the bending of light off the optical axis.

As seen from Fig. 3, the three lens designs vary not only in bending angle, but also in light distribution and intensity. We measured the fraction of the energy passing through the slits of the three lenses (T_1) as well as the fraction of the energy reaching the region of interest (T_2). The EM wave intensity is quantitatively proportional to the square of the amplitude of electric field; however, as the magnetic field is proportional to the electric field and there is only one magnetic field component with incident TM waves, we will use the square of the magnetic field to represent the intensity in all subsequent calculations [31]. For all proposed lenses, the magnitude of the magnetic field was captured along the output surface of the lenses. To find

#134990 - $15.00 USD Received 13 Sep 2010; revised 11 Oct 2010; accepted 15 Oct 2010; published 22 Oct 2010

T_1, the square of this field was integrated along the surface and divided by the integral of the input intensity over a geometrically equivalent surface. And T_2 was the ratio of the maximum intensity along the focal direction to the incident intensity. The measured efficiencies are listed in Table 1.

Table 1. Efficiency calculation of the proposed plasmonic lenses.

	Lens I	Lens II	Lens III
Efficiency of energy passing through the lenses (T_1)	62.16%	40.48%	72.27%
Efficiency of focusing (T_2)	19.36%	6.25%	20.25%

We observe that T_1 is significantly higher than T_2 in all cases. The major reason is that in plasmonic waveguides the decoupling rate of plasmonic modes into propagating EM wave modes is low. Most of the energy remains at the output surface of the lens in the form of propagating surface plasmons, which circumvent the singularities at the sharp corners of the slits. The existence of those surface plasmon waves can be confirmed by observing the region between the slits near the output plane of the lenses in Fig. 3. Thus, an intuitive approach to improve the efficiency of focusing is to increase the roughness of the output surface, which will cause more energy decouple into light and propagate to the far field.

Although the bending angle of the focused beam by Lens III is a little smaller than that by Lens I, the design of tapered apertures in Lens III renders better efficiency of focusing. As reported previously [21], tapered structures, with its ability to collect input light and confine plasmonic modes, can produce extraordinary optical transmission. This observation matches well with our simulation results (see Table 1). We observe that Lens II produces weaker light intensity (Fig. 3(d)) than those in Lens I (Fig. 3(b)) and Lens III (Fig. 3(f)). This observation is likely caused by two factors: the smaller input apertures of Lens II, and the slanted output plane introducing additional phase changes (expressed in Eq. (2)), which could cause some destructive interference at the focal point decreasing the intensity.

In the simulation shown in Fig. 3, the incident light is normal to lens surface. We proceed to investigate the lens performance when the EM waves are incident at an angle to the optical axis (Fig. 4). In Fig. 4(a), light impinges on Lens III at an angle of −10° to the optical axis (y = 0). Such a condition adds an extra planar phase front that interferes with the asymmetric phase front of the plasmonic lens, leading to a larger bending angle off the axial direction. Figure 4(b) shows that the bending angle increases from 5° to 17°. In this case, the beam can be shifted nearly 1 μm in the y-direction, which is large enough for applications such as plasmonic communications and nanofabrication. Our simulation results also indicate that when the incident angle is 10° above the optical axis (Fig. 4(c)), the light beam is deflected toward the optical axis, but not enough to cross it. The deflection angle is observed to be −6° (Fig. 4(d)).

The slits used in our three plasmonic lens designs are either rectangular or trapezoid. These plain geometries guarantee the simplicity in fabrication using the FIB technique. One can imagine that a plasmonic lens with continuously varying tapered slits would act differently and perhaps achieve better efficiency and larger bending effect than those of the proposed lenses. The tapered lenses with curved surfaces, however, bring complexity to fabrication and thus are not investigated in this manuscript. In addition, the proposed lenses may be further optimized by fine-tuning the geometrical parameters (such as width, length, and spacing of the slits).

#134990 - $15.00 USD Received 13 Sep 2010; revised 11 Oct 2010; accepted 15 Oct 2010; published 22 Oct 2010

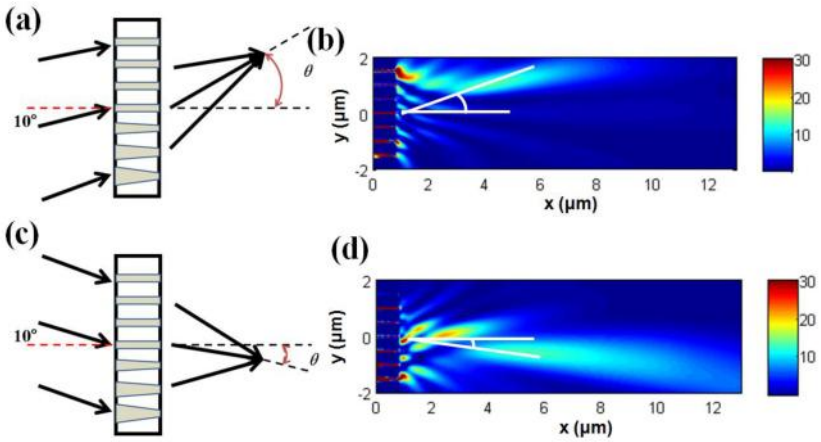

Fig. 4. Influence of different incident angles on the bending effects of Lens III. The red dashed lines denote the phase front change caused by both incident light and plasmonic lenses. (a) Schematic of light incidence at an angle of −10° to the optical axis; (b) Simulation results corresponding to (a). (c) Schematic of light incidence at an angle of 10° to the optical axis. (d) Simulation results corresponding to (c).

5. Conclusion

We have designed three different plasmonic lens structures to achieve the directional tuning of light. Based on our FDTD simulation, when the incident light is normal to the lens surface, deflection angles of 8°, 3°, and 5° in the far field have been achieved in the three designs, respectively. We also show that with light incident at 10° below the optical axis, a deflection up to 17° in the far field can be achieved. Compared with existing plasmonic lenses [16, 17] that can bend light, our lens designs have advantages in ease of fabrication and capability to perform in the far field. With these advantages, we expect our plasmonic lenses to be valuable in applications such as plasmonic circuits and photonic communication.

Acknowledgment

We gratefully acknowledge the financial support from Air Force Office of Scientific Research (AFOSR), National Science Foundation (NSF), and the Penn State Center for Nanoscale Science (MRSEC).

#134990 - $15.00 USD Received 13 Sep 2010; revised 11 Oct 2010; accepted 15 Oct 2010; published 22 Oct 2010